

Fellenius, B.H. and Rahman, M.M., 2019. Load-movement response by t-z and q-z functions. Geotechnical Engineering Journal of the SEAGS & AGSSEA Journal, September 2019, 50(3) 11-19.

Load-movement Response by t-z and q-z Functions

Bengt H. Fellenius¹ and Mohammad Manzur Rahman²

¹Consulting Engineer, Sidney, BC, Canada, V8L 2B9. E: bengt@fellenius.net

²Civil Engineering Division, Bangladesh Water Development Board, Motijheel, Dhaka-1000, Bangladesh
E-mail: maruf.ce2k7@gmail.com

ABSTRACT. A static loading test provides more than a single-point value, "capacity". The primary use of a loading test is to show the load-movement response of the pile-and-soil system in order to assist in analysis of the transfer of a supported load to the soil. A pile is composed of a series of short lengths (elements) that are affected by shaft shear or toe stress, expressed as a relation of stress (load) versus movement for the element. The response of the soil around a pile element is expressed in load-transfer functions. The response of a pile head, that is, the actual pile load-movement curve, is the sum of the response of a series of individual pile elements. Fitting the theoretical load-movement response to actual test results by trial-and-error applying a series of shaft (t-z) functions and a toe (q-z) function, enables a calibration of a pile and site that serves to establish the load-transfer conditions of a piled foundation needed for determining what short and long-term settlement the foundation will experience. Thus, a crude "capacity" assessment will not do. Eight functions for modeling strain-hardening and strain-softening response are presented in the paper and their use in fitting theoretical to actual results is illustrated.

KEYWORDS. Load-movement response, t-z and q-z function, Test simulation.

1. INTRODUCTION

The design of a piled foundation involves assessing and optimizing three factors: safety, serviceability, and economy. Simply basing the design on ratio between capacity (or ultimate resistance) and the working load is not satisfactory. First, because there is little consensus of what constitutes capacity. Indeed, the capacity defined according to the method preferred by one engineer can differ by a factor of two from that considered by another engineer (Fellenius 2013a; 2017) and, also, because the assessed capacity is quite dependent on how the static loading test was performed. Second, because determining a working load by downgrading the assessed capacity using some safety factor or resistance factor says little how the pile will respond to that working load. Instead, the results of a static loading test should be assessed in terms of the pile load-movement response. The assessment, or back-analysis starts by fitting a theoretical simulation of the measured load-movement, the results of which allows for assessing how the pile will respond to applied load from a structure.

The fitting makes use of the fact that a pile can be considered to be an axial unit composed of a series of short lengths (elements) that are affected by shaft shear or toe stress. The simulation then applies relations of load or stress versus movement for the elements. The load-movement of the pile head combines (integrates) the response of the elements and pile shortening (or lengthening for a tension case). The pile-element relation is called load-transfer function (also called t/z/q-z curve), which is a mathematical expression of the load and movement relation. All load-transfer functions are curves that either rise steeply at first and become less steep as the movement increases or reduce after having reached a peak at a certain movement. On occasions, a shaft resistance is constant after having reached a maximum value, thus, exhibiting a plastic response. However, the load movement response for shaft resistance along a pile element (after an initial movement) is only rarely plastic, more often, it is either strain-hardening or strain-softening, and a pile-toe element will always show a strain-hardening response.

A load-transfer function expresses the load as a function of a movement per some non-linear mathematical relation further affected by a "function coefficient" that, sometimes with an additional parameter, control the shape of the curve. Fitting a load-transfer function to an actual test is best carried out by selecting a specific load, a "Target Point", on the test curve, a "Target Load" at a "Target Movement", as outlined below.

2. MATHEMATICAL RELATIONS

Several t-z/q-z relations have been proposed to model the load-movement response of pile element. Eight are presented in this paper as showing the load as governed by movement and as correlated to a selected Target Load and a Target Movement. The Target can be, but is not usually the estimated "capacity" (ultimate resistance) of the load-movement response.

2.1 Chin (1970)

A hyperbolic relation is the most common approximation of a stiffening shear-resistance load-movement response (also called strain-hardening) of an element. It is most often expressed in the "Chin-Kondner" function shown by Eqs. 1a to 1c. Some define the load at infinite movement as the ultimate resistance of the element. It is approached asymptotically and can be considered akin to a plastic response after a large movement. The slope of the straight line of Movement/Load (δ_n/Q_n) versus Movement (δ_n) expresses the resistance mobilized at infinite movement.

$$Q_n = \frac{\delta_n}{C_1 \delta_n + C_2} \quad (1a)$$

$$C_1 = 1/Q_{inf} \quad (1b)$$

$$C_2 = \delta_n \left(\frac{1}{Q_n} - \frac{1}{Q_{inf}} \right) \quad (1c)$$

Where

- Q_n = applied load
- δ_n = movement paired with Q_n
- C_1 = function coefficient ($= 1/Q_{inf}$), which is also the slope of the straight line in the δ/Q versus movement, δ .diagram
- C_2 = y-axis intercept of the C_1 -slope
- Q_{inf} = load at infinite movement

2.2 Decourt (1999; 2008)

Equations 2a and 2b show a hyperbolic relation similar to that of Chin (1970) as proposed by Decourt (1999; 2008). When applied to a back-calculation of actual test data, it gives essentially the same fit and the load at infinite movement is often also considered to be the ultimate resistance of the element. That load is also the intersection of the straight line of Load/Movement over Movement (Q_n/δ_n) versus Load (Q_n).

$$Q_n = \frac{C_2 \delta_n}{1 - C_1 \delta_n} \quad (2a)$$

$$Q_{inf} = \frac{C_2}{C_1} \quad (2b)$$

Where Q_n = applied load
 δ_n = movement paired with Q_n
 C_1 = function coefficient. Also the slope of the straight line in the Q_n/δ_n versus movement diagram
 C_2 = y-intercept of the straight line in the Q/δ versus movement diagram
 Q_{inf} = load at infinite movement

2.3 Gwizdala (1996)

Equation 3 shows a strain-hardening function proposed Gwizdala (1996) that is particularly useful for modeling a pile toe response. The function is also called "Ratio" or "Power" function. The function states that the ratio between a load, Q_n , to any other load, herein called "Target Load", Q_{trg} , is equal to the ratio of the movements of these loads, δ_n and δ_{trg} raised to an exponent, θ , the "function coefficient", that can range from zero through unity. Setting the function coefficient to unity results in a straight line. In contrast to the hyperbolic function, the load at infinite movement of the Gwizdala function is infinitely large.

$$Q_n = Q_{trg} \left(\frac{\delta_n}{\delta_{trg}} \right)^\theta \quad (3)$$

Where Q_n = applied load
 δ_n = movement paired with Q_n
 Q_{trg} = target load or resistance
 δ_{trg} = target movement (mobilized at Q_{trg})
 θ = function coefficient; an exponent; $0 \leq \theta \leq 1$

2.4 Van der Veen (1953)

Equation 4 shows a function proposed by Van der Veen (1953) that displays a plastic response after an initial rise to a maximum value, the "Target Load", Q_{trg} . The function coefficient, b , determines the movement at the target load. (The van der Veen function is sometimes called the "exponential function"; rather a misnomer).

$$Q_n = Q_{trg} (1 - e^{-b\delta_n}) \quad (4)$$

Where Q_n = applied load
 δ_n = movement paired with Q_n
 Q_{trg} = target load or resistance
 b = function coefficient > 0

2.5 Hansen (1963)

Equations 5a through 5c are strain-softening functions proposed by Hansen (1964). A strain-softening function shows a curve that first increases to a maximum or peak value (Q_{peak}), then, at some movement, reduces (softens) with further movement.

$$Q_n = \frac{\sqrt{\delta_n}}{C_1 \delta_n + C_2} \quad (5a)$$

$$Q_{peak} = \frac{1}{2\sqrt{C_1 C_2}} \quad (5b)$$

$$\delta_{peak} = \frac{C_2}{C_1} \quad (5c)$$

Where Q_n = applied load
 δ_n = movement paired with Q_n
 C_1 = function coefficient; also the slope of the straight line of $Movement^{0.5}/Load$ vs. $Movement$ ($\delta_{0.5}/Q_n$ vs. δ_n).
 C_2 = y-axis intercept of the C_1 -slope; must be > 0
 Q_{peak} = peak load
 δ_{peak} = movement paired with Q_{peak}

2.6 Zhang and Zhang (2012)

Equations 6a through 6c are strain-softening functions proposed by Zhang and Zhang (2012).

$$Q_n = \frac{\delta_n (a + c\delta_n)}{(a + b\delta_n)^2} \quad (6a)$$

$$Q_{peak} = 1/(4b-c) \quad (6b)$$

$$\delta_{peak} = \frac{a}{b-2c} \quad (6c)$$

Where A_n = applied load
 a_n = movement paired with A_n
 a = function coefficient
 b = parameter = $(1/2Q_{peak} - a/\delta_{peak})$
 c = parameter = $(1/4Q_{peak} - a/\delta_{peak})$
 P_{peak} = peak load
 δ_{peak} = movement paired with P_{peak}

2.7 Vijayvergiya (1977)

Equation 7 shows a strain-softening function proposed by Vijayvergiya (1977). The Vijayvergiya function coefficient, V , ranges from unity to about 5. It controls the shape of the curve before and after the target movement. For a V -coefficient equal to 2.0, the curve reaches a peak at the target movement, which makes it convenient to assume that an ultimate resistance has been reached at the target point. However, this is only valid if the Target Load is the peak value and, thus, the continued response of the test curve is truly strain-softening. For V -coefficients larger than 2.0, a Vijayvergiya curve shows a peak load that is larger than the Target Load occurring at a movement smaller than the Target Movement. For $V = 1$, the function becomes a Gwizdala function with a function coefficient, θ , of 0.5. At $V = 0$, Eq. 7 describes a straight line.

$$Q_n = Q_{trg} \left(V \sqrt{\frac{\delta_n}{\delta_{trg}}} - (V-1) \frac{\delta_n}{\delta_{trg}} \right) \quad (7)$$

Where Q_n = applied load
 δ_n = movement paired with Q_n
 Q_{trg} = target load or resistance
 δ_{trg} = target movement (paired with Q_{trg})
 V = function coefficient; > 0

2.8 Rahman (2018)

Equation 8 shows a function proposed by the second author. The function equation includes two function coefficients, One denoted "M" and one denoted "F". Usually, in fitting to an actual load-movement curve, M and F range from about 1.0 through 3.0 and 1.5 through 2.0, respectively.

$$Q_n = Q_{trg} \left(\frac{\delta_{trg} \delta^{F-1} + \delta_{trg}^{F-1} \delta_n}{\delta_{trg}^F + \delta_n^F} \right)^{\frac{1}{M}} \tag{8}$$

Where Q_n = applied load
 δ_n = movement paired with Q_n
 Q_{trg} = target load or resistance
 δ_{trg} = target movement (paired with Q_{trg})
 V = function coefficient; > 0
 F = function coefficient; > 1.0

3. FUNCTION CURVES FOR COMMON TARGETS

When a static loading test is carried out on a instrumented pile, the test results include measurements of axial load determined at strain-gage locations at various depths, each being the records of a pile element. When studying the load-movement response as measured for an element, it is convenient to normalize the load and movement data to percent of a selected target point. The "Target Load" on the ordinate and "Target Movement" on the abscissa have then coordinates of 100 % and 100%, respectively.

Figure 1 compares the normalized Chin-Kondner (hyperbolic) and Figure 2 the Gwizdala (ratio) function. That is, the two functions that represent strain-hardening response. For both, all of the function curves go through the respective Target Point. The function coefficients (C_1 and θ , respectively) control the shape of the respective curve before and after the Target Point. The Chin function coefficient, C_1 , ranges from a low of 0.0010 through a high of 0.0095 and the Gwizdala coefficient, θ , ranges from a low of 0.05 through a high of 1.00. The 0.0060 C_1 -coefficient and the 0.20 θ -coefficient are typical for the two functions, respectively, for fitting to an actual shaft resistance response, although, the Gwizdala function is rarely suitable for modeling of shaft resistance. The Gwizdala function is usually the best for fitting a simulation to measured toe resistance. The coefficient, θ , is then usually larger than 0.50. The exception is when the fit is to measurements of toe response affected by residual force.

By choosing a function coefficient close to 0.0100, the Chin-Kondner hyperbolic function can be used to simulate an essentially elastic-plastic response, thus, avoiding having to use a two-line curve where the change between elastic and plastic response is in the form of a kink.

Figure 3 shows the van der Veen function. For a function coefficient, b , equal to 0.10, the Target Load and Target Movement are both 100 %. For b smaller than 0.10, reaching the target requires movement larger than the 100% Target Movement, while curves with b larger than 0.10 reach the Target Load at a movement smaller than the 100% Target Movement. Similar to the Chin function, choosing a van der Veen function coefficient, b , larger than about 0.2, can be used to simulate an essentially elastic-plastic response to an imposed load.

Figure 4 shows the Vijayvergiya strain-softening curves. For function coefficients, V , equal to 2.0, the peak load is the Target Load. However, for coefficients other than 2.0, the curves always reach a peak that is larger than the Target Load and they occur before the 100-% Target Movement. For function coefficients (V) smaller than

2.0, it would seem that the function ceases to be strain-softening. This is only apparent, they just reach the peak at a movement larger than the maximum of the abscissa scale. The Vijayvergiya function is usually used with the function coefficient, V , of 2.0. It is only rarely applied with a V -range outside 1.75 through 2.25.

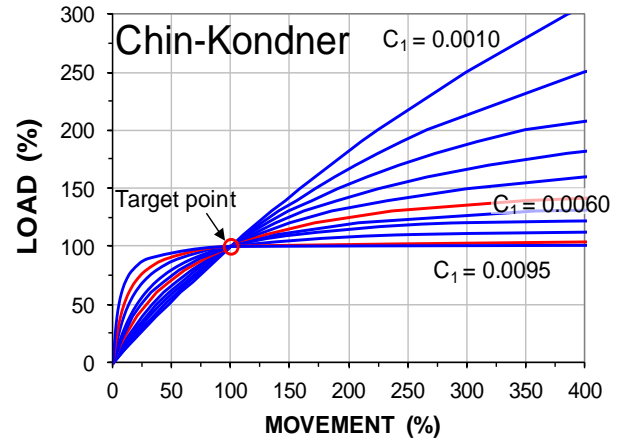


Figure 1 Load-transfer curves per the Chin-Kondner (1970)

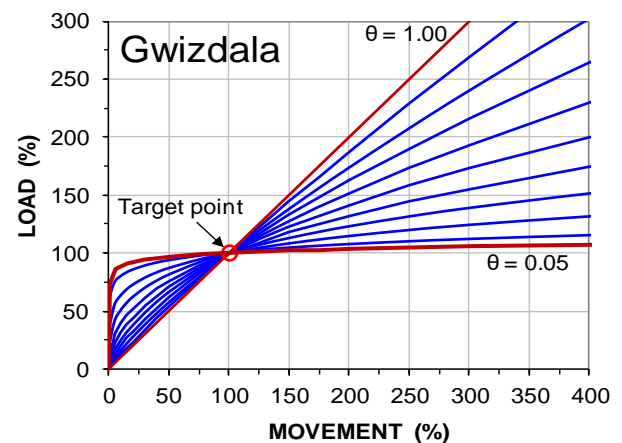


Figure 2 Load-transfer curves per the Gwizdala (1996)

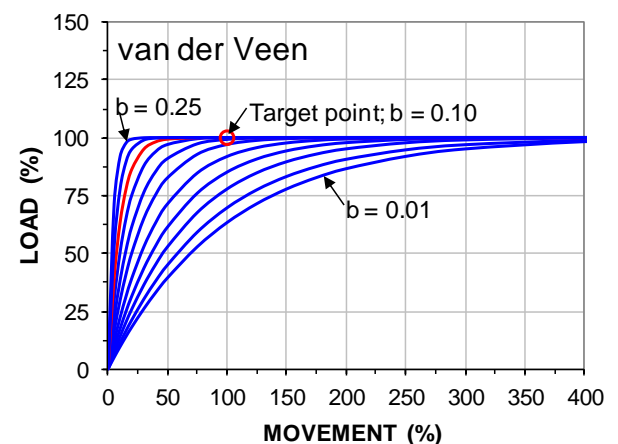


Figure 3 Load-transfer curves per the van der Veen (1953)

Figure 5 shows the Hansen strain-softening functions. Unlike the Vijayvergiya function, the maximum load will always be the 100 % value. The function coefficient, C_1 , controls the shape of the curve

and the magnitude of the movement at the target load. At $C_1 = 0.0005$, the movement is equal to the 100-% target movement.

Choosing a coefficient smaller than 0.0005 will represent a t-z curve for which the target load is mobilized at a movement smaller than that at the 100-% Target Movement, while choosing C_1 larger than 0.00050, the Target Load is mobilized at a movement larger Target Movement. For both options of a coefficient not being 0.0005, the load calculated at 100-% movement will be smaller than the target load.

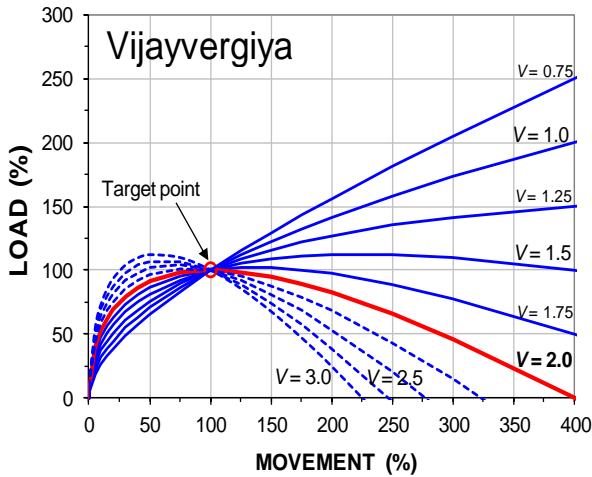


Figure 4 Load-transfer curves per the Vijayvergiya (1977)

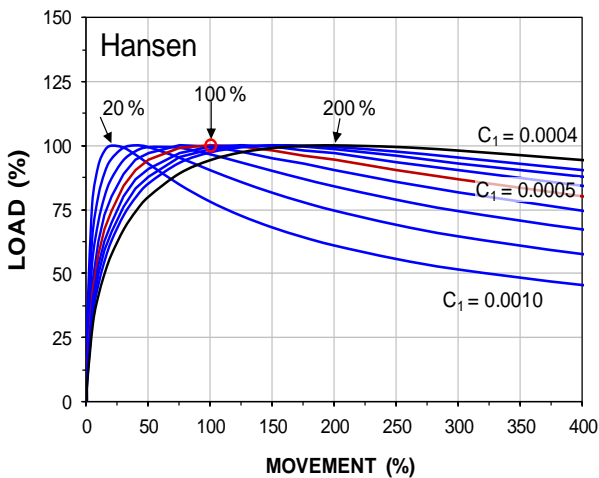


Figure 5 Load-transfer curves per the Hansen (1977)

Figure 6 shows the Zhang strain-softening functions. In contrast to the Hansen function, all curves go through the target point (100% load and 100% movement) and the function coefficient, a , just controls the shape of the curves. Thus, the Zhang function is often easier to use than the Hansen function, when fitting results to a known target point where the issue is the shape of the t-z curve before and after the target point.

Rahman strain-softening function is governed by two coefficients, M , and F . In fitting to an actual case, the trial-and-error procedure is to keep one of the two constant, while adjusting the other. Figure 7a shows the Rahman curves for a fixed function coefficient, $M = 1.00$, and a range of function coefficients, F , and Figure 7b shows a fixed function coefficient, $F = 2.00$, and a range of function coefficients, M . In fitting to actual test records, it is most practical to start with $F = 2$ and, then, when having obtained a reasonably good fit by varying " M ", fine-tune the fit by means of varying F , while keeping M unchanged.

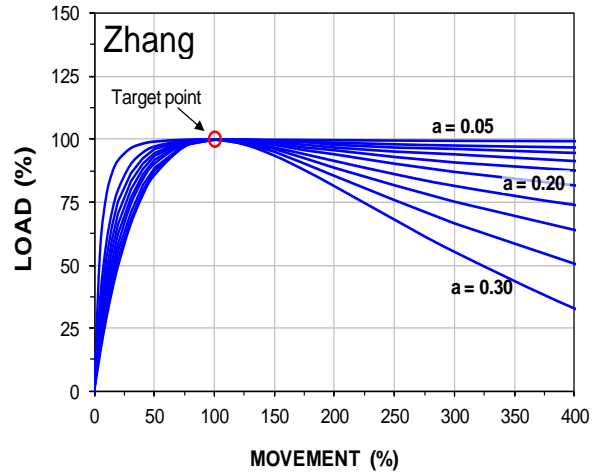


Figure 6 Load-transfer curves per the Zhang and Zhang (1977)

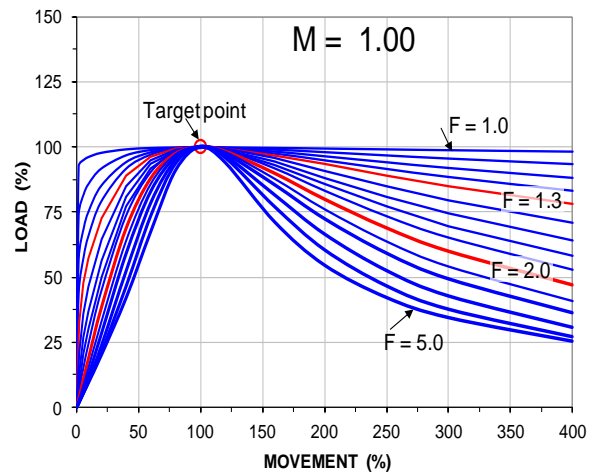


Figure 7a Load-transfer curves per Rahman (2018)

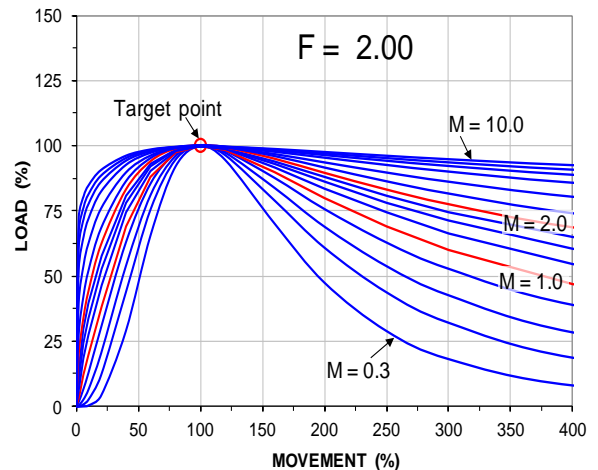


Figure 7b Load-transfer curves per Rahman (2018)

4. CASE HISTORY APPLICATION

In simulation of load-movement response measured in actual full-scale tests, usually one of the cited functions will produce a better fit than another. In the following, the functions are applied to actual test results on an 800 mm diameter bored pile in a fine-grained soil published by Bohn et al. (2017)

Figures 8 and 9 show shaft-resistance movement curves from static loading test measured at two separate pile elements in the test pile. Both examples indicate strain-softening shaft resistance response. Figure 8 shows a peak resistance at a movement of no more than 5 mm, while for the test plotted in Figure 9 shows no peak before the movement relative the pile and the soil was 20 mm. Back-calculations attempting to obtain a best-fit for each of the eight t-z functions to the measured curves show a reasonable to excellent fit for the curve portion before the peak resistance for all but the Hansen and Vijayvergiya functions. Of course, the three strain-hardening functions, Chin-Kondner, Decourt, and Gwizdala, cannot show any agreement to the post-measured peak resistance, which is the obvious case also for the van der Veen function with its plastic post-peak response. Neither was it possible to obtain a good post-peak fit of the Hansen and Vijayvergiya strain-softening functions. However, for both examples, the Zhang and Rahman functions gave a good fit to the measured load-movement throughout. Indeed, the Rahman fit is excellent.

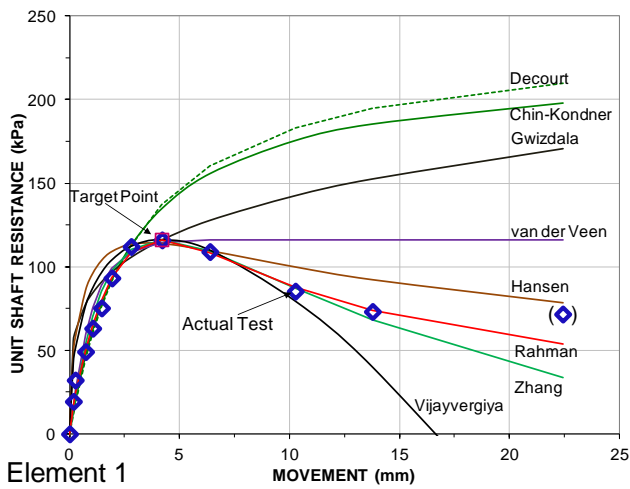


Figure 8 Best-fit functions actual records of unit shaft resistance along a Pile Element 1

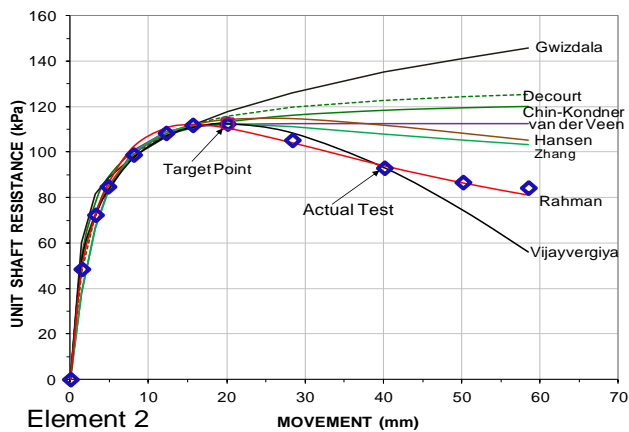


Figure 9 Best-fit functions actual records of unit shaft resistance along a Pile Element 2

The curves shown in Figures 8 and 9 make it clear that for any meaningful conclusion to be drawn from a fit between a function curve and an actual test curve requires that the data and the closeness of the fit between calculated to measured must go well past a peak value.

Figures 10 and 11 show results from the pile-head load-movement measured in a bidirectional test (O-cell test; Osterberg 1989) on an 1,800-mm diameter, 50 m deep bored pile (Loadtest 2015) in Sioux City, Idaho.

For the downward load-movement of the lower length of the test pile (Figure 8), it was not possible to fit a single t-z function to the full length of the lower portion of the test pile. A function that fitted a first portion did not fit the second. To obtain the best fit of the Gwizdala and Chin-Kondner strain-hardening curves, required considering two portions of the curve, a first portion and a second, each with its own target point. The reason was that the downward load-movement response was the effect of both shaft and toe resistance. The trial-and-error fits included adjusting the soil strength parameters (beta-coefficients) for the individual soil layers, still ensuring that the target load, which is a sum of all element loads, stayed the one selected.

For the upward portion (Figure 9), the response was from shaft resistance only and, because the shaft resistance was fairly similar soil (sand and silt) along the upper length of the pile, both the Gwizdala and Chin-Kondner strain-hardening functions gave good fits. The figure also shows the fits of the van der Veen and the Vijayvergiya and Rahman strain-softening functions, which could only be made to fit an initial portion of the upward load-movement curve (all three had the same Target Load). The Vijayvergiya function could be made to fit the entire record, but, as the Target Load then had to be input as larger than the maximum test load and the function coefficient be reduced to a value of 1.0, the fit has little meaning.

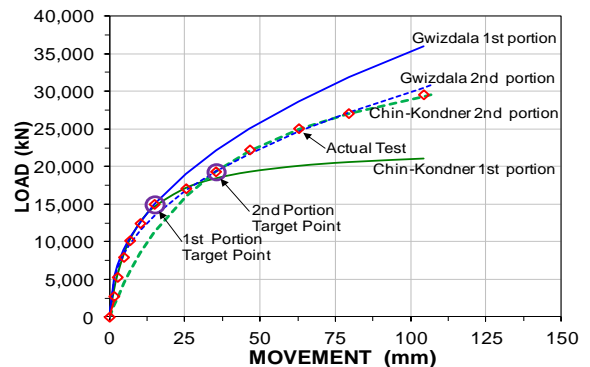


Figure 10 Measured and simulated strain-hardening downward curve, load-movements (Data from Loadtest 2015)

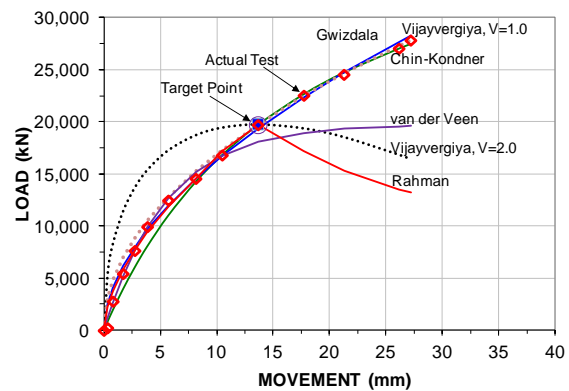


Figure 11 Measured and simulated strain-hardening upward curve, load-movements, Sioux City, IH. (Data from Loadtest 2015)

Obviously, fitting to the load-movement of a pile, as opposed to a pile element, omits influence of pile shortening (pile compression) and the fact that shaft resistance response for shaft elements and the pile toe are quite different.

Figure 12 show the results of applying a t-z analysis to the pile shaft elements and the pile-toe element and fitting the load-movement of the individual element together with the pile shortening to obtain the load-movement measured at the bidirectional cell level. The shaft resistance was modeled using a Chin-Kondner hyperbolic function and the toe resistance was modelled using a Gwizdala function. The simulation was made using the UniPile5 software (Goudreault and Fellenius 2014).

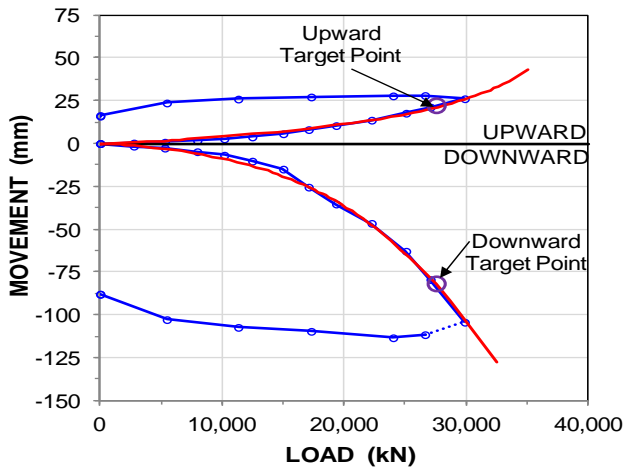


Figure 12 Upward and downward measured and fitted bidirectional (O-cell) curves. Test in Sioux City, IH. (Data from Loadtest 2015)

The downward and upward load-movement curves of the bidirectional test are often combined to provide an equivalent head-down test. Most often, the equivalent test curve is constructed mechanically and directly from the test records with adjustment to the fact that the load affecting the pile below the depth of the bidirectional cell, BD, will have caused an axial pile shortening between the pile head and the BD depth. However, this approach neglects the fact that the upward portion of the bidirectional test will first engage the soil nearest the BD level and the soil nearest the pile will be engaged last. In the head-down test, the opposite occurs. Moreover, the upward curves—both measured and fitted—include the pile weight, whereas for the head-down load-movement (and the bidirectional downward curve), the influence of the pile weight is not included. Thus, the mechanical and direct method will result in an equivalent pile-head load-movement curve that is stiffer than the true head-down load-movement curve, which can easily lead to an overestimation of the test results.

Figure 13 shows the equivalent head-down load-movement curves determined by applying the same t-z element functions in simulating the head-down static loading test of the Sioux City test. The diagram illustrates results of different ways to extrapolate the test data from a known load-movement point. The point usually of primary interest is the point on the pile head load-movement curve that represents the value of the sum of the downward and upward loads (with due adjustment of the pile weight for the latter) marked "Head at twice the max. test load". Pile head load-movement beyond this point is an extrapolation of the test data.

However, the advantage of the bidirectional test over a head-down test is that the mobilization of the pile toe is to a much larger load and movement than in the equivalent head-down test to a load equal to twice the cell load. The point "Head at maximum toe movement" indicates the pile head load that would be required to mobilize the pile toe to a load-movement equal to that in the test.

The profession has different opinions about what pile-head load of the equivalent pile-head load-movement curve that represents the pile "capacity" of the test. However, this difference of opinions is rather irrelevant for structures supported on the test pile and, therefore, also to the design of the piled foundation. What matters is the settlement of the foundation supporting under the working load.

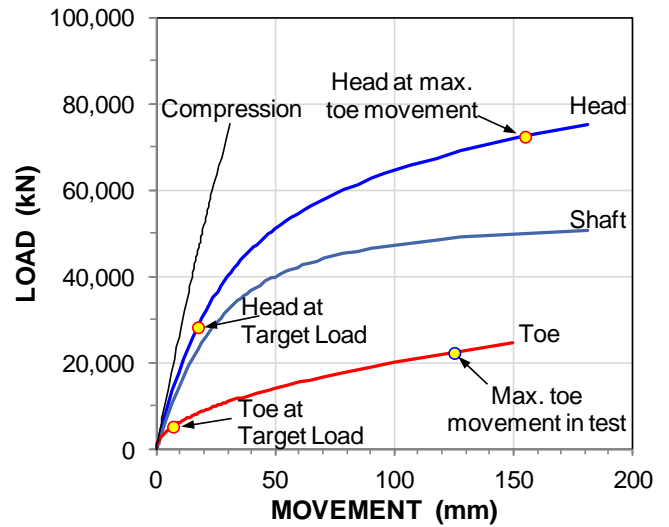


Figure 13 Equivalent head-down load-movement curves

Figure 14 shows the load distribution for the target load of the analysis determined directly from the fitting process. Additional distributions for a larger or smaller load applied to the pile head can easily be produced. The figure represents the simulation of the shaft resistance after adjustment for pile weight. It is simple to consider the effect of placing a working load at the pile head and to simulate the subsequent load distribution for the short- and long-term conditions to arrive at a decision as to accept or not the working load for the pile from the aspect of settlement. It is beyond the scope of this paper to indicate the process. Such details have been presented by Fellenius (2016a). The primary conclusion is that applying the t-z functions to analyse the results of the static loading test enables determining the settlement of the foundation supported on the pile and removes the need for involving an irrelevant assessment of "capacity" and applying some "factor of safety" or "resistance factor" to arrive at a presumed "safe" working load that may or may not introduce an acceptable level of settlement.

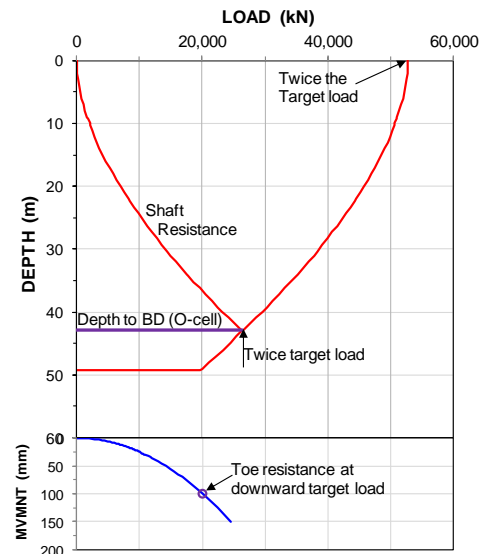


Figure 14 Load-distributions for the Target Load (Test in Sioux City, Idaho)

Figure 15 shows results of a bidirectional test in silty sand carried out in Brazil (Elisio 1983), which involves measuring the upward movement of the pile head and the downward movement of the cell level. The pile was a 700-mm diameter, 11.5 m long, full-displacement pile. For the piles shorter than about 15 m, adding instrumentation for measuring pile shortening (additional telltales) and load distribution (strain-gage instrumentation) is usually superfluous. In contrast, had the test been a head-down test, instrumentation would have been necessary in order to determine the load distribution and, in particular, the pile toe response. The same process was applied of selecting target point on the curve and fitting simulated upward and downward load-movement curves using t-z functions for shaft element and the pile toe by means of a trial-and-error using the UniPile5 software. (N.B., the upward and downward target loads for the upward and downward curves are equal, but the target movements differ).

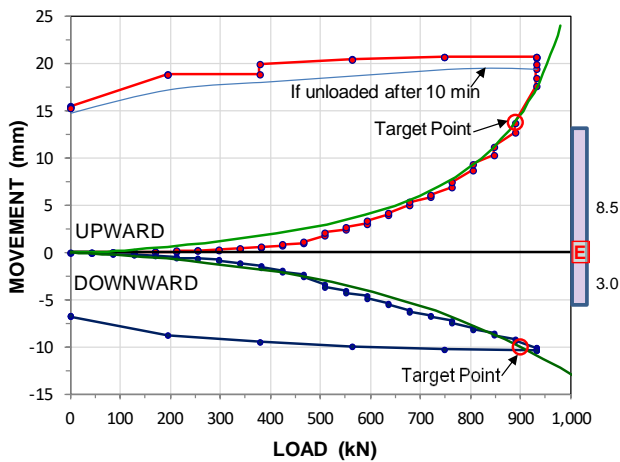


Figure 15 Results of a bidirectional test at tower and shopping center, Sao Paulo, Brazil (Fellenius 2014; data courtesy of Arcos Engenharia de Solos, Brazil)

Figure 16, presents the equivalent head-down load-movement curves, as determined by the UniPile5 software applying the same t-z functions as used for the fitting to the bidirectional test. Again, the specific points of interest are marked out in the diagram.



Figure 16 Equivalent head-down load-movement for tower and shopping center, Sao Paulo, Brazil (Fellenius 2014)

Figure 17 shows the equivalent head-down load-distribution, as determined by the UniPile5 software applying the same t-z functions as used for the fitting to the bidirectional test determined applying the

same soil parameters and t-z functions as used for the fitting to the bidirectional test).

Figure 18 shows results of another bidirectional test carried out in Brazil. The pile was a 400-mm diameter, 16.0 m long, full-displacement pile, and the soil profile consisted of sandy clay turning to sandy silt. The figure includes the results of applying a t-z analysis to the pile shaft elements and the pile-toe element and fitting the load-movement of the individual element together with the pile shortening to obtain the load-movement measured at the bidirectional cell level. The shaft resistance was modelled using a van der Veen function along the length above the BD and a Chin-Kondner function along the length below. The toe resistance was modelled using a Gwizdala function. The simulation fit was made using the UniPile5 software (Goudreault and Fellenius 2014).

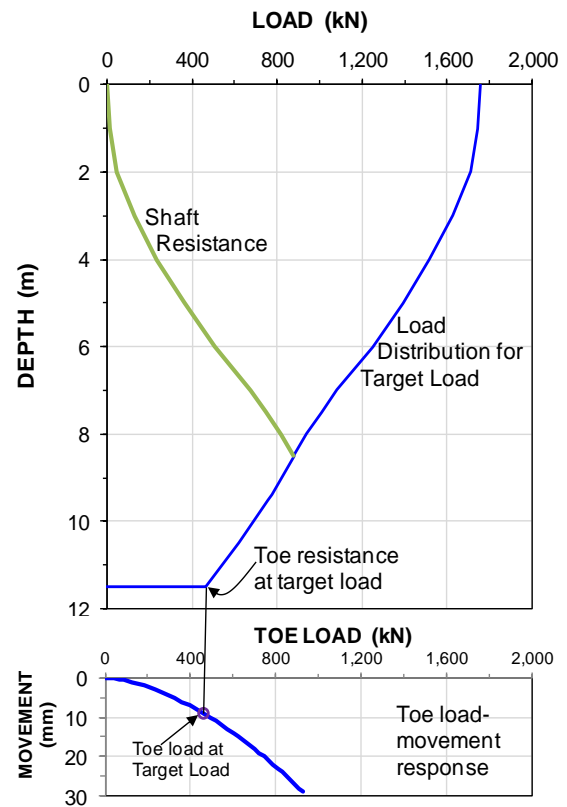


Figure 17 Equivalent head-down load-movement for tower and shopping center, Sao Paulo, Brazil (Fellenius 2014)

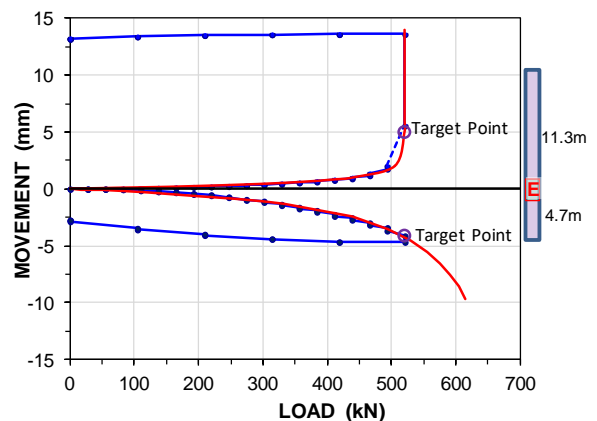


Figure 18 Results of a bidirectional test at tower and shopping center, Belo Horizonte, Brazil. (Fellenius 2014; data courtesy of Arcos Engenharia de Solos, Brazil)

Figure 19 shows the equivalent head-down load-movement curves, as determined applying the same t-z functions as used for the fitting to the bidirectional test.

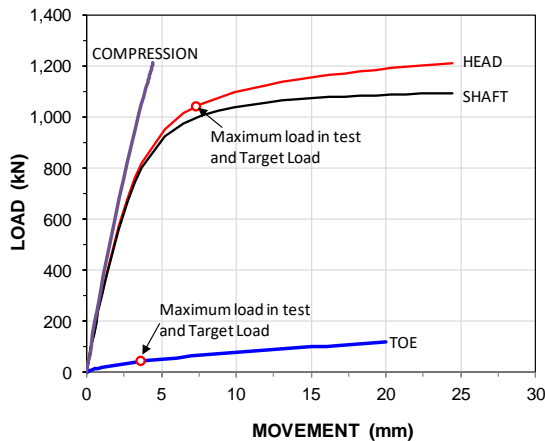


Figure 19 Equivalent head-down load-movement at tower and shopping center, Belo Horizonte, Brazil (Fellenius 2014)

Figure 20 shows the equivalent head-down load distribution for the Target Point analysis. It is obvious that the pile toe resistance is very small. The load-distribution analysis will enable an estimate to be made of the long-term settlement of a pile foundation supported on similar pile for which the analysis of the pile response would have to include the effect of adjacent foundation and other influencing factors (Fellenius 2016a).

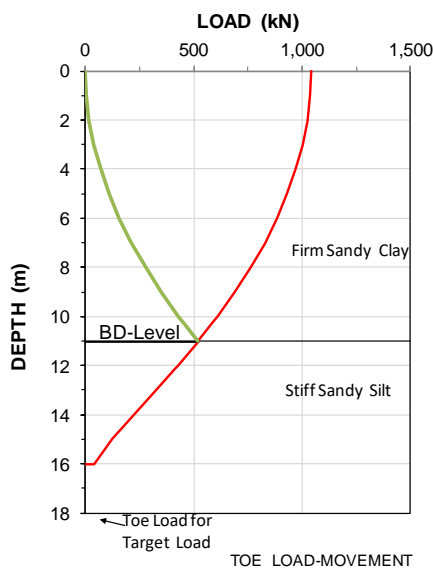


Figure 20 Equivalent head-down load distribution at tower and shopping center, Belo Horizonte, Brazil (Fellenius 2014)

5. CONCLUSIONS

In fitting a calculated (simulated) t-z curve to a measured response of a pile element, e.g., strain-gage records from an instrumented pile, it is important that the set of records covers the full mobilization of the gage level as demonstrated in Figure 7. A back-calculation only addressing an initial portion of the records can achieve an "excellent agreement" using any functions, but has then limited value.

Nothing is gained or learnt by fitting a load-transfer function to a pile-head load-movement response. This is because the response is a summary of the responses of the series of individual pile elements

along the shaft and the toe element plus the 'elastic' shortening of the pile shaft. A characteristic point on the pile head load-movement curve, such as peak load, does not occur at the same time as similar characteristic points occur at the series of pile elements representing the pile.

A load-transfer back-calculation does not require imposing an assumed ultimate resistance. Such items or issues are unrelated to the load-transfer functions. This notwithstanding that a couple of the load-transfer functions can be used as reference to ultimate resistance. It is a futile effort to define a pile capacity as a sum of ultimate shear along pile elements, defined one way or another, and combined with a perceived ultimate toe resistance. Those values will not develop simultaneously or occur for the same load applied by the pile head jack (or bidirectional cell). (Besides, the capacity value obtained from accumulating element responses will not be the same as a capacity determined from the pile-head load-movement curve). The useful approach is to base the analysis on load-transfer functions acting at a series of pile elements. It enables a design to be carried out that addresses settlement of the single pile and pile group, the more realistic issue in piled foundation design.

Not only will the end results enable a settlement analysis of the pile represented by the test pile, when the t-z function(s) that fit the conditions for the pile and the soil have been established, the effect of shortening or lengthening a pile, of using a pile with a larger or smaller diameter, of excavating around the piles or adding fill to the site, etc. can be determined.

The trial-and-error fitting process can be speeded up by using the Excel spreadsheet template published by the first author (Fellenius 2016b).

On establishing in a back-calculation fit to measured pile element responses (i.e., records from the gage locations), then, a suitable computer program needs to be engaged to combine the response of all the elements making up the pile, for example, the UniPile5 software (Goudreault and Fellenius 2014), and to calculate the resulting pile head (and pile toe movement) for use, say, in settlement analysis of a foundation supported on the piles, as recommended by Fellenius (2016a).

6. REFERENCES

- Bohn, C., Lopes dos Santos, A., and Frank R., 2017. Development of axial pile load transfer curves based on instrumented load tests. *ASCE J. of Geotechnical and Geoenviron. Engng.*, 143(1) 15 p.
- Chin, F.K., 1971. Discussion on pile test. Arkansas River project. *ASCE Journal for Soil Mechanics and Foundation Engineering*, 97(SM6) 930-932.
- Decourt, L., 1999. Behavior of foundations under working load conditions. *Proc. of 11th Pan-American Conference on Soil Mechanics and Geotechnical Engineering, Foz DoGuassu, Brazil, August 1999, Vol. 4, pp. 453-488.*
- Decourt, L., 2008. Loading tests: interpretation and prediction of their results. *ASCE GeoInstitute Geo-Congress New Orleans, March 9-12, Honoring John Schmertmann—From Research to Practice in Geotechnical Engineering, Geotechnical Special Publication, GSP 180, Edited by J.E. Laier, D.K. Crapps, and M.H. Hussein, pp. 452-488.*
- Elisio, P.C.A.F., 1983. *Celula Expansiva Hidrodinamica—Uma nova maneira de executar provas de carga (Hydrodynamic expansive cell. A new way to perform loading tests). Independent publisher, Belo Horizonte, Minas Gerais State, Brazil, 106 p.*
- Fellenius, B.H., 2013a. Capacity and load-movement of a CFA pile: A prediction event. *ASCE GeoInstitute Geo Congress San Diego, March 3-6, 2013, Foundation Engineering in the Face of Uncertainty, ASCE, Reston, VA, James L. Withiam, Kwok-Kwang Phoon, and Mohamad H. Hussein, eds., Geotechnical Special Publication, GSP 229, pp. 707-719.*

- Fellenius, B.H., 2013b. Simplified non-linear approach for single pile settlement analysis. Discussion. Canadian Geotechnical Journal, 50(6) 685-687.
- Fellenius, B.H., 2014. Analysis of results from routine static loading tests with emphasis on the bidirectional test. Proceedings of the 17th Congress of the Brasileiro de Mecanica dos Solos e Engenharia, Cobramseg, Goiania, Brazil, September 10 - 13, 22 p.
- Fellenius, B.H., 2016a. The unified design of piled foundations. The Sven Hansbo Lecture. Geotechnics for Sustainable Infrastructure Development—Geotec Hanoi 2016, edited by Phung Duc Long, Hanoi, November 23-25, pp. 3-28.
- Fellenius, B.H., 2016b. An Excel template crib sheet for use with UniPile and UniSettle. www.Fellenius.net.
- Fellenius, B.H., 2017. Report on the prediction survey of the 3rd Bolivian International Conference on Deep Foundations. Proceedings, Santa Cruz de la Sierra, Bolivia, April 27-29, Vol. 3, pp. 7-25.
- Goudreault, P.A. and Fellenius, B.H., 2014. UniPile Version 5, User and Examples Manual. Geotechnical Solutions Ltd. [www.UniSoftLtd.com]. 120 p.
- Gwizdala, K., 1996. The analysis of pile settlement employing load-transfer functions (in Polish). Zeszyty Naukowe No. 532, Budownictwo Wodne No.41, Technical University of Gdansk, Poland, 192 p.
- Hansen, J.B., 1963. Discussion on hyperbolic stress-strain response. Cohesive soils. ASCE Journal for Soil Mechanics and Foundation Engineering, 89(SM4) 241- 242.
- Loadtest Inc. 2015. TS1, I-29 Bridge over Floyd River, Sioux City, IA, Drilled shaft test Osterberg method, Report LT-1289, May 17, 2015, 123 p.
- Osterberg, J., 1989. New device for load testing driven piles and bored piles separates friction and end-bearing. Deep Foundations Institute, Proc. of the International Conference on Piling and Deep Foundations, London, London June 2-4, Eds. J.B. Burland and J.M. Mitchell, A.A. Balkema, Vol. 1, pp. 421–427.
- Vander Veen, C., 1953. The Bearing Capacity of a Pile. Proceedings of the 3rd ICSMFE, Zurich, Switzerland, August 16-27, Vol. 2, pp. 84-90.
- Vijayvergiya, V.N., 1977. Load-movement characteristics of piles. Ports '77: 4th Annual Symposium of the Waterway, Port, Coastal, and Ocean Division, ASCE, Los Angeles, 269-284.
- Zhang Q.Q. and Zhang, Z.M., 2012. Simplified non-linear approach for single pile settlement analysis. Canadian Geotechnical Journal, 49(11) 1256-1266.